SIAM J. SCI. COMPUT.
Vol. 38, No. 6, pp. A3492–A3514

ROBUST PRECONDITIONING FOR XFEM APPLIED TO TIME-DEPENDENT STOKES PROBLEMS*

SVEN GROSS†, THOMAS LUDESCHER†, MAXIM OLSHANSKII‡, AND ARNOLD REUSKEN†

Abstract. We consider a quasi-stationary Stokes interface problem with a reaction term proportional to $\tau = 1/\Delta t \geq 0$ as obtained by a time discretization of a time-dependent Stokes problem. The mesh used for space discretization is not aligned with the interface. We use the P_1 extended finite element space for the pressure approximation and the standard conforming P_2 finite element space for the velocity approximation. A pressure stabilization term known from the literature is added, since the FE pair is not LBB stable. For the stabilized discrete bilinear form we derive a new inf-sup stability result. A new Schur complement preconditioner is proposed and analyzed. We present an analysis which proves robustness of the preconditioner with respect to h, τ, with $\tau \in [0, c_0] \cup [c_1 h^{-2}, \infty)$, and the position of the interface. Numerical results are included which indicate that the preconditioner is robust for the whole parameter range $\tau \geq 0$ and also with respect to the viscosity ratio μ_1/μ_2.

Key words. Schur complement preconditioning, Stokes equations, interface problem, extended finite elements, stabilization

AMS subject classifications. 65N15, 65N22, 65N30, 65F10

DOI. 10.1137/15M1024007

1. Introduction.

In this paper we treat a Stokes problem on a bounded connected polygonal domain Ω in d-dimensional Euclidean space ($d = 2, 3$), which is partitioned into two connected subdomains Ω_i, $i = 1, 2$. For simplicity we assume that Ω_1 is strictly contained in Ω. The interface between the two subdomains is denoted by Γ, i.e., $\Gamma = \partial\Omega_1$. The normal at Γ is denoted by n_Γ. On each of the two subdomains we assume given constant strictly positive values for density ρ_i and viscosity μ_i and consider the following problem: Find a velocity vector field u and a pressure function p such that

$$\begin{aligned} \tau\rho_i u - \operatorname{div}(\mu_i D(u)) + \nabla p &= f_1 && \text{in } \Omega_i, \quad i = 1, 2, \\ \operatorname{div} u &= 0 && \text{in } \Omega_i, \quad i = 1, 2, \\ [u] &= 0 && \text{on } \Gamma, \\ [-p n_\Gamma + \mu D(u) n_\Gamma] &= f_2 && \text{on } \Gamma, \\ u &= 0 && \text{on } \partial\Omega, \end{aligned} \tag{1.1}$$

with $\tau \geq 0$ a given constant, $D(u) := \nabla u + (\nabla u)^T$, and $[v]$ denotes the jump of the quantity v across the interface Γ. Our interest in problem (1.1) is motivated

*Submitted to the journal's Methods and Algorithms for Scientific Computing section June 1, 2015; accepted for publication (in revised form) August 22, 2016; published electronically November 1, 2016.

http://www.siam.org/journals/sisc/38-6/M102400.html

Funding: The second author's work was partially supported by the DFG through grant RE 1461/6-1. The third author's work was partially supported by the NSF through the Division of Mathematical Sciences grants 1315993 and 1522192.

†Institut für Geometrie und Praktische Mathematik, RWTH-Aachen, D-52056 Aachen, Germany (gross@igpm.rwth-aachen.de, thomas.ludescher@rwth-aachen.de, reusken@igpm.rwth-aachen.de).

‡Department of Mathematics, University of Houston, Houston, TX 77204 (molshan@math.uh.edu).

by the numerical simulation of two-phase Navier–Stokes equations [15]. After time discretization one obtains a quasi-stationary problem of the form (1.1), where f_1 accounts for inertia terms and external forcing and f_2 are surface tension forces. The jump in normal stress at the interface results in a *discontinuity of the pressure* across Γ. Below we shall introduce a well-posed weak formulation of this problem, in which the condition $[u] = 0$ is treated as an essential condition in the choice of the trial space and the condition on the normal stresses is treated as a natural interface condition. In two-phase flow applications the interface is unknown and finding its location is a part of the numerical simulation. Thus often the fluid dynamics problem is coupled with an interface capturing technique. One commonly used interface capturing technique is the level set method; see [28, 8, 24] and the references therein. If the level set method is used, then typically in the discretization of the flow equations the interface is *not aligned* with the grid. This causes certain difficulties with respect to an accurate discretization of the flow variables. Recently, extended finite element methods (XFEM) have been developed to obtain accurate finite element discretizations; see, for example, [10, 17, 15, 7]. These methods are closely related to the so-called CutFEM; cf. [5]. We consider one particular XFEM, in which the pressure variable is approximated in a conforming P_1-XFE space and the velocity is approximated in the standard conforming P_2-FE space. This pair of spaces is popular in the discretization of two-phase incompressible flows [13, 25, 26]. The pair is not LBB stable and therefore a stabilization technique is needed. We use the stabilization suggested in [17]. In the recent report [18], this finite element discretization method has been analyzed for the stationary variant of (1.1), i.e., $\tau = 0$. For the corresponding variational formulation, an inf-sup stability result is derived with the key property that the stability constant is *uniform with respect to h, the viscosity quotient μ_1/μ_2, and the position of the interface in the triangulation.* Based on this result and interpolation error estimates, optimal discretization error bounds are derived in [18]. We use this discretization for the quasi-stationary problem (1.1). After discretization one obtains a symmetric saddle point system. Due to the use of the standard P_2-FE space for the velocity, optimal preconditioners for the velocity block in the stiffness matrix are known (e.g., multigrid). In [18] a robust Schur complement preconditioner for the stationary case ($\tau = 0$) is presented. In this paper, we derive a new Schur complement preconditioner for the quasi-stationary case ($\tau \geq 0$). We propose a preconditioner that is *robust with respect to h, τ, μ_1/μ_2, and the position of the interface in the triangulation.*

The three main contributions of this paper are the following. First, we present a Schur complement preconditioner that is new. Second, for a part of the parameter range, namely, $\tau \in [0, c_0] \cup [c_1 h^{-2}, \infty)$, with constants $c_i > 0$, we give a theoretical analysis from which the robustness property follows. For our analysis, we need an LBB type stability result for the Darcy limit, i.e., $\tau \to \infty$. We prove this new result (3.2). Finally, we give results of systematic numerical experiments, which indicate that the robustness property of the preconditioner holds for the whole parameter range $\tau \geq 0$, and propose a slight modification of the Schur complement preconditioner which has improved robustness with respect to the density ratio ρ_1/ρ_2.

2. Discrete problem: P_2-P_1XFEM pair. For the finite element method we first introduce a suitable weak formulation of (1.1). For a subdomain ω of Ω the L^2 scalar product on ω is denoted by $(\cdot,\cdot)_{0,\omega}$. We use the notation $(\cdot,\cdot)_0 := (\cdot,\cdot)_{0,\Omega}$. The piecewise constant functions μ, ρ are defined by $\mu(x) = \mu_i$, $\rho(x) = \rho_i$ for $x \in \Omega_i$. We

introduce the spaces $V := H_0^1(\Omega)^d$, $Q := \{\, p \in L^2(\Omega) \mid \int_\Omega \mu^{-1} p(x)\, dx = 0 \,\}$ and the bilinear forms

$$a(u,v) := \frac{1}{2}\int_\Omega \mu D(u) : D(v)\, dx, \quad b(v,p) = -(\operatorname{div} v, p)_0.$$

The weak formulation reads as follows: Given $f \in V'$ find $(u,p) \in V \times Q$ such that

$$\begin{cases} a(u,v) + \tau(\rho u, v)_0 + b(v,p) = f(v) & \forall\ v \in V, \\ b(u,q) = 0 & \forall\ q \in Q. \end{cases} \tag{2.1}$$

The functional f contains contributions from both the volume force f_1 and the surface force f_2 in (1.1). We refer to the literature for a derivation of this weak formulation, which is well-posed [11, 15].

Assume a family of shape regular quasi-uniform triangulations consisting of simplices $\{\mathcal{T}_h\}_{h>0}$. The triangulations are not fitted to the interface Γ. Corresponding to the family of triangulations, we assume a family of discrete surfaces $\{\Gamma_h\}_{h>0}$ approximating Γ. Each Γ_h is a $C^{0,1}$ surface and can be partitioned into planar segments (line segments for $d = 2$, triangles or quadrilaterals for $d = 3$), consistent with the outer triangulation $\mathcal{T}_h$, i.e., for any $T \in \mathcal{T}_h$ an intersection $T \cap \Gamma_h$ either is planar or has zero $(d-1)$-measure. We assume that Γ_h is close to Γ in the following sense:

$$\operatorname*{ess\,sup}_{x \in \Gamma_h} |n(x) - n_h(x)| \leq c\, h, \tag{2.2}$$

where n is the extension of n_Γ in a neighborhood of Γ and n_h is a unit normal on Γ_h. Since the rest of the paper deals with a discrete problem, in what follows and without ambiguity, Ω_1 and Ω_2 denote the interior and the exterior of Γ_h rather than of Γ. The coefficients ρ_i, μ_i are assumed to be piecewise constant with respect to this mesh-dependent partition Ω on Ω_1 and Ω_2.

We introduce the subdomains

$$\Omega_{i,h} := \{\, T \in \mathcal{T}_h \mid \operatorname{meas}_d(T \cap \Omega_i) > 0 \,\}, \quad i = 1,2,$$

and the corresponding standard linear finite element spaces

$$Q_{i,h} := \{\, v_h \in C(\Omega_{i,h}) \mid v_h|_T \in \mathcal{P}_1 \ \ \forall\ T \in \Omega_{i,h} \,\},\ i = 1,2.$$

We use the same notation $\Omega_{i,h}$ for the set of simplices as well as for the subdomain of Ω which is formed by these simplices, as its meaning is clear from the context. For the stabilization procedure that is introduced below we need a further partitioning of $\Omega_{i,h}$. Define the set of elements intersected by Γ_h,

$$\mathcal{T}_h^\Gamma := \{\, T \in \mathcal{T}_h \mid \operatorname{meas}_{d-1}(T \cap \Gamma_h) > 0 \,\},$$

and let

$$\omega_{i,h} := \Omega_{i,h} \setminus \mathcal{T}_h^\Gamma, \quad i = 1,2.$$

Note that $\mathcal{T}_h = \omega_{1,h} \cup \omega_{2,h} \cup \mathcal{T}_h^\Gamma$ holds and forms a disjoint union. The corresponding sets of faces (needed in the stabilization procedure) are given by

$$\mathcal{F}_i = \{\, F \subset \partial T \mid T \in \mathcal{T}_h^\Gamma, \ \ F \not\subset \partial\Omega_{i,h} \,\}, \ \ i = 1,2,$$

and $\mathcal{F}_h := \mathcal{F}_1 \cup \mathcal{F}_2$. For each $F \in \mathcal{F}_h$ a fixed orientation of its normal is chosen and the unit normal with that orientation is denoted by n_F. These definitions are illustrated, for $d = 2$, in Figure 1.

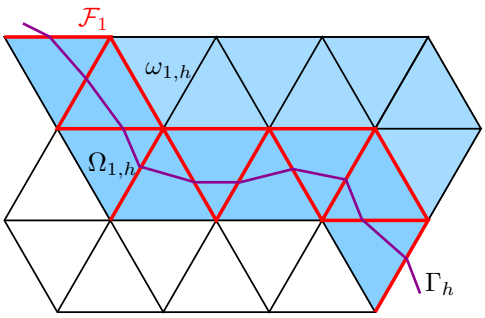

FIG. 1. *Set of faces $\mathcal{F}_1$ (in red) and subdomains $\omega_{1,h}$ (light blue) and $\Omega_{1,h}$ (light and darker blue triangles) for a two-dimensional example.*

A given $p_h = (p_{1,h}, p_{2,h}) \in Q_{1,h} \times Q_{2,h}$ may have two values, $p_{1,h}(x)$ and $p_{2,h}(x)$, for $x \in \mathcal{T}_h^\Gamma$. We define a univalued function $p_h^\Gamma \in C(\Omega_1 \cup \Omega_2)$ by

$$p_h^\Gamma(x) = p_{i,h}(x) \quad \text{for } x \in \Omega_i.$$

PROPOSITION 2.1. *The mapping $p_h \mapsto p_h^\Gamma$ is bijective.*

Proof. Surjectivity holds by construction. Assume $p_h, q_h \in Q_{1,h} \times Q_{2,h}$ with $p_h \neq q_h$. Without loss of generality we can assume $p_{1,h} \neq q_{1,h}$. There exists $T \in \Omega_{1,h}$ such that $q_{1,h} \neq p_{1,h}$ a.e. on T. By the definition of $\Omega_{1,h}$, we have that $\text{meas}_d(T \cap \Omega_1) > 0$. Hence $q_h^\Gamma = (q_h)_{|\Omega_1} \neq (p_h)_{|\Omega_1} = p_h^\Gamma$ on a subset of Ω_1 with positive measure. This proves injectivity. ∎

On $Q_{1,h} \times Q_{2,h}$ we use a norm denoted by $\|p_h\|^2_{0,\Omega_{1,h}\cup\Omega_{2,h}} := \|p_{1,h}\|^2_{0,\Omega_{1,h}} + \|p_{2,h}\|^2_{0,\Omega_{2,h}}$. The XFEM space of piecewise linears is defined by

$$Q_h := (Q_{1,h} \times Q_{2,h})/\mathbb{R} = \{\, p_h \in Q_{1,h} \times Q_{2,h} \mid (\mu^{-1} p_h^\Gamma, 1)_0 = 0 \,\}. \tag{2.3}$$

The space Q_h is used for the discretization of the pressure. Note that $\{\, p_h^\Gamma \mid p_h \in Q_h \,\}$ is a subspace of the pressure space Q.

For the velocity discretization we use the standard conforming P_2-space

$$V_h := \{\, v_h \in C(\Omega)^d \mid v_{h|T} \in \mathcal{P}_2^d \ \ \forall\, T \in \mathcal{T}_h,\ v_{|\partial\Omega} = 0 \,\} \subset H_0^1(\Omega)^d.$$

The pair $V_h \times Q_h$ is not uniformly LBB stable with respect to how the interface Γ_h cuts through the triangulation; cf. [15]. Hence, we need a pressure stabilization. For this we introduce the bilinear form

$$\begin{aligned} j(p_h, q_h) &:= \sum_{i=1}^{2} j_i(p_{i,h}, q_{i,h}), \quad p_h, q_h \in Q_{1,h} \times Q_{2,h}, \\ \text{with } j_i(p_{i,h}, q_{i,h}) &:= \mu_i^{-1} \sum_{F \in \mathcal{F}_i} h_F^3([\nabla p_{i,h} \cdot n_F], [\nabla q_{i,h} \cdot n_F])_{0,F}, \end{aligned} \tag{2.4}$$

which is also referred to as a ghost penalty term; cf. [4]. Here $[\nabla p_{i,h} \cdot n_F]$ denotes the jump of the normal component of the piecewise constant function $\nabla p_{i,h}$ across the face F. Since $p_{i,h} \in Q_{i,h}$ is continuous in $\Omega_{i,h}$, i.e., the tangential component of $\nabla p_{i,h}$ has no jump across $F \in \mathcal{F}_i$, we replace $[\nabla p_{i,h} \cdot n_F]$ by $[\nabla p_{i,h}]$ (to simplify the notation).

The discretization of (2.1) that we consider is as follows: determine $(u_h, p_h) \in V_h \times Q_h$ such that

(2.5)
$$k\big((u_h,p_h),(v_h,q_h)\big) = f(v_h) \quad \text{for all } (v_h,q_h) \in V_h \times Q_h,$$
$$k\big((u_h,p_h),(v_h,q_h)\big) := a(u_h,v_h) + b(v_h,p_h^\Gamma) + \tau(\rho u_h, v_h)_0 + b(u_h,q_h^\Gamma) - \varepsilon_p j(p_h,q_h),$$

with a sufficiently large stabilization parameter $\varepsilon_p \geq 0$, independent of τ, h, and how Γ_h intersects the mesh. In [18] this finite element discretization method was analyzed for the stationary case, i.e., $\tau = 0$. A uniform LBB type stability result and on optimal order error estimates were derived. In this paper, we prove a different uniform inf-sup stability result for the pair of finite element spaces and, based on this result, we focus on developing a robust preconditioner for the algebraic problem.

3. LBB type stability conditions. In [18] the following LBB type inequality was derived:

$$\sup_{v_h \in V_h} \frac{(\operatorname{div} v_h, p_h^\Gamma)_0}{\|\mu^{\frac12}\nabla v_h\|_0} + \left(\sum_{i=1}^2 \sum_{F\in\mathcal{F}_i} h^3 \|\mu_i^{-\frac12}[\nabla p_{i,h}]\|_{0,F}^2\right)^{\frac12} \gtrsim \|\mu^{-\frac12} p_h\|_{0,\Omega_{1,h}\cup\Omega_{2,h}} \tag{3.1}$$

for all $p_h \in Q_h$. This result forms the basis for the analysis of the Schur complement preconditioner for the case $\tau = 0$ in [18]. Here and in the remainder of this paper we use the notation $A \gtrsim B$ when $A \geq c\,B$ holds with a positive constant c independent of h, the problem parameters ρ, μ, and how Γ_h intersects the triangulation. Similarly, $A \lesssim B$ is defined and $A \simeq B$ obviously means that both $A \gtrsim B$ and $A \lesssim B$ hold.

The goal of this section is to prove the alternative LBB type stability property

$$\begin{aligned}\sup_{v_h \in V_h} \frac{(\operatorname{div} v_h, p_h^\Gamma)_0}{\|\rho^{\frac12} v_h\|_0} + \left(\sum_{i=1}^2 \sum_{F\in\mathcal{F}_i} h \|\rho_i^{-\frac12}[\nabla p_{i,h}]\|_{0,F}^2\right)^{\frac12} \\ \gtrsim \|\rho^{-\frac12}\nabla p_h^\Gamma\|_{0,\Omega_1\cup\Omega_2} + \rho_{\max}^{-\frac12} h^{-\frac12}\|[p_h^\Gamma]\|_{0,\Gamma_h} \quad \forall\, p_h \in Q_{1,h}\times Q_{2,h},\end{aligned} \tag{3.2}$$

where $[p_h^\Gamma] := (p_{1,h} - p_{2,h})_{|\Gamma_h}$ denotes the interfacial jump of p_h^Γ and $\rho_{\max} = \max\{\rho_1,\rho_2\}$. Recall that the P_2-P_1XFEM pair (V_h, Q_h) is not LBB stable. The second term on the left-hand side is a ghost penalty stabilization as in (2.4), though with a different h-scaling. We split the proof of (3.2) into two partial results in the next two lemmata.

LEMMA 3.1. *The following uniform bound holds for $i = 1, 2$:*

$$\sup_{\substack{v_h \in V_h \\ \operatorname{supp}(v_h)\subset\Omega_i}} \frac{(\operatorname{div} v_h, p_h^\Gamma)_0}{\|v_h\|_0} + \left(\sum_{F\in\mathcal{F}_i} h\|[\nabla p_{i,h}]\|_{0,F}^2\right)^{\frac12} \gtrsim \|\nabla p_h^\Gamma\|_{0,\Omega_i} \quad \forall\, p_h \in Q_{i,h}. \tag{3.3}$$

Proof. For any two tetrahedra $T_1, T_2 \in \Omega_{i,h}$ sharing a face F, the regularity of triangulation assumption yields the estimate

$$\|\nabla p_{i,h}\|_{0,T_1}^2 \lesssim \|\nabla p_{i,h}\|_{0,T_2}^2 + h\|[\nabla p_{i,h}]\|_{0,F}^2.$$

Applying the above inequality to estimate $\|\nabla p_{i,h}\|_{0,T}^2$ over all $T \in \mathcal{T}_h^\Gamma$, and using the fact that any $T \in \mathcal{T}_h^\Gamma$ can be reached starting from a suitable tetrahedron in $\omega_{i,h}$ crossing a finite independent of h number of faces from $\mathcal{F}_i$, we obtain the estimate

$$\sum_{F\in\mathcal{F}_i} h\|[\nabla p_{i,h}]\|_{0,F}^2 + \|\nabla p_{i,h}\|_{0,\omega_{i,h}}^2 \geq c\,\|\nabla p_{i,h}\|_{0,\Omega_{i,h}}^2 \geq c_0\|\nabla p_h^\Gamma\|_{0,\Omega_i}^2. \tag{3.4}$$

(This estimate was introduced in the analysis of a stabilized Nitsche method for the Poisson and Stokes equations in [6, 22].) Let $V_h(\omega_{i,h})$ be the velocity FE space on the triangulation $\omega_{i,h} \subset \Omega_i$ (zero values on $\partial\omega_{i,h}$). From the literature [3] the following inf-sup property of the Hood–Taylor P_2-P_1 pair is known:

$$\sup_{v_h\in V_h(\omega_{i,h})} \frac{(\operatorname{div} v_h, p_{i,h})}{\|v_h\|_{0,\omega_{i,h}}} \geq c_i\|\nabla p_{i,h}\|_{0,\omega_{i,h}} \quad \forall\ p_{i,h} \in Q_{i,h} \tag{3.5}$$

with $c_i > 0$ independent of h. We square (3.5), scale with c_i^{-2}, and combine it with (3.4) to obtain

$$c_i^{-2} \sup_{v_h\in V_h(\omega_{i,h})} \frac{(\operatorname{div} v_h, p_{i,h})^2}{\|v_h\|_{0,\omega_{i,h}}^2} + \sum_{F\in\mathcal{F}_i} h\|[\nabla p_{i,h}]\|_{0,F}^2 \geq c_0\|\nabla p_h^\Gamma\|_{0,\Omega_i}^2.$$

Simple calculations yield (3.3). ∎

We need to derive a uniform bound for the second term on the right-hand side of (3.2). This is done in Lemma 3.2. For the proof of that lemma we need some special decomposition of the surface Γ_h, which we now introduce. We start with the decomposition of Γ_h into the set of (planar) segments $\mathcal{F}_\Gamma := \{F := \Gamma_h \cap T \mid T \in \mathcal{T}_h^\Gamma\}$:

$$\Gamma_h = \bigcup_{F\in\mathcal{F}_\Gamma} F.$$

A subset of "large" surface segments is defined by

$$\mathcal{F}_\Gamma^0 := \{F \in \mathcal{F}_\Gamma \mid \operatorname{meas}_{d-1}(F) \geq \gamma_0 h^{d-1}\}$$

with a suitable constant γ_0. Proposition 4.2 from [9] implies that there exist constants $\gamma_0 > 0$ and $c > 0$ depending on the shape regularity of the outer triangulation $\mathcal{T}_h$, but independent of h and of how Γ_h intersects the mesh, such that for each $F \in \mathcal{F}_\Gamma$ there exists an $F^0 \in \mathcal{F}_\Gamma^0$ satisfying

$$\operatorname{dist}(F, F^0) \leq c\,h. \tag{3.6}$$

For every $\Gamma_h \cap T = F \in \mathcal{F}_\Gamma^0$ let $\mathrm{b}(F)$ be the barycenter of F and $\mathrm{v}(F) \in \partial T$ a vertex of T that is closest to $\mathrm{b}(F)$. Let $\phi(F)$ be the scalar nodal linear finite element basis function corresponding to the vertex $\mathrm{v}(F)$. Let $\widetilde{\mathcal{F}}_\Gamma^0$ be a maximal subset of $\mathcal{F}_\Gamma^0$ such that $\operatorname{supp}(\phi(F)) \cap \operatorname{supp}(\phi(\tilde{F})) = \emptyset$ for any $F, \tilde{F} \in \widetilde{\mathcal{F}}_\Gamma^0$, $F \neq \tilde{F}$. The property (3.6) also holds with the set $\mathcal{F}_\Gamma^0$ replaced by the smaller set $\widetilde{\mathcal{F}}_\Gamma^0$ (and a possibly larger constant c). The elements in $\widetilde{\mathcal{F}}_\Gamma^0$ are labeled by an index set K, i.e., $\widetilde{\mathcal{F}}_\Gamma^0 = \{F_k \mid k \in K\}$. Each $F \in \mathcal{F}_\Gamma \setminus \widetilde{\mathcal{F}}_\Gamma^0$ is added to the (or one of the) surface segments $F_k \in \widetilde{\mathcal{F}}_\Gamma^0$ which has smallest distance to F. The resulting enlarged surface macro elements are denoted by $\tilde{F}_k$.

This results in a decomposition of Γ_h with the following properties:

$$\begin{cases} \Gamma_h = \bigcup_{k\in K} \tilde{F}_k, \quad \mathrm{int}(\tilde{F}_k)\cap \mathrm{int}(\tilde{F}_j) = \emptyset \quad \text{if } k \neq j, \\ \forall\, k \in K \;\; \exists\, F_k \in \mathcal{F}_\Gamma^0 \;\; \text{such that } F_k \subset \tilde{F}_k, \\ |\tilde{F}_k| \simeq h^{d-1}, \quad \mathrm{diam}(\tilde{F}_k) \lesssim h \quad \forall\, k \in K. \end{cases}$$

LEMMA 3.2. *There exists $h_0 > 0$ such that for all $h \le h_0$ the uniform bound*

$$\sup_{v_h\in V_h} \frac{(\mathrm{div}\, v_h, p_h^\Gamma)_0}{\|v_h\|_0} + \left(\sum_{i=1}^2 \sum_{F\in\mathcal{F}_i} h \|[\nabla p_{i,h}]\|_{0,F}^2 \right)^{\frac12} \gtrsim h^{-\frac12} \|[p_h^\Gamma]\|_{0,\Gamma_h} \tag{3.7}$$

for all $p_h \in Q_{1,h} \times Q_{2,h}$ holds.

Proof. For a given $p_h \in Q_{1,h} \times Q_{2,h}$, introduce the notation $q = [p_h^\Gamma]$. We thus have

$$h^{-1}\|[p_h^\Gamma]\|_{0,\Gamma_h}^2 = h^{-1} \int_{\Gamma_h} q^2\, dx = h^{-1} \sum_{k\in K} \int_{\tilde{F}_k} q^2\, dx.$$

Let $\mathrm{b}_k = \mathrm{b}(F_k)$ be the barycenter of a large surface element $F_k \subset \tilde{F}_k$ (as explained above). For $x \in \tilde{F}_k$ let $\int_{\mathrm{b}_k}^x \nabla q \cdot t\, ds$ be the line integral along the shortest path in $\tilde{F}_k$ which connects b_k and x. Here t denotes the tangential unit vector along this path. The domain formed by the simplices in $\mathcal{T}_h^\Gamma$ that are intersected by the macro surface segment $\tilde{F}_k$ is denoted by $\mathcal{T}_k^\Gamma$. Note that $|\mathcal{T}_k^\Gamma| \simeq h^d$ holds. Using this, $\|x - \mathrm{b}_k\| \lesssim h$, and the estimate in (3.4) we get

$$\begin{aligned} h^{-1} \sum_{k\in K} \int_{\tilde{F}_k} \left| \int_{\mathrm{b}_k}^x \nabla q \cdot t\, ds \right|^2 dx &\lesssim h \sum_{k\in K} |\tilde{F}_k| \sum_{i=1}^2 \|\nabla p_{i,h}\|_{L^\infty(\tilde{F}_k)}^2 \\ &\lesssim h^d \sum_{k\in K} \sum_{i=1}^2 \|\nabla p_{i,h}\|_{L^\infty(\tilde{F}_k)}^2 \lesssim \sum_{k\in K} \sum_{i=1}^2 \int_{\mathcal{T}_k^\Gamma} |\nabla p_{i,h}|^2\, dx \\ &\lesssim \sum_{i=1}^2 \|\nabla p_{i,h}\|_{0,\Omega_{i,h}}^2 \lesssim \sum_{i=1}^2 \|\nabla p_{i,h}\|_{0,\omega_i}^2 + \sum_{i=1}^2 \sum_{F\in\mathcal{F}_i} h \|[\nabla p_{i,h}]\|_{0,F}^2 \\ &\lesssim \|\nabla p_h^\Gamma\|_{0,\Omega_1\cup\Omega_2}^2 + \sum_{i=1}^2 \sum_{F\in\mathcal{F}_i} h \|[\nabla p_{i,h}]\|_{0,F}^2. \end{aligned} \tag{3.8}$$

Using $q(x) = q(\mathrm{b}_k) + \int_{\mathrm{b}_k}^x \nabla q \cdot t\, ds$ we obtain

$$\begin{aligned} h^{-1}\|[p_h^\Gamma]\|_{0,\Gamma_h}^2 &\le 2h^{-1} \sum_{k\in K} |\tilde{F}_k|\, q(\mathrm{b}_k)^2 + 2h^{-1} \sum_{k\in K} \int_{\tilde{F}_k} \left| \int_{\mathrm{b}_k}^x \nabla q \cdot t\, ds \right|^2 dx \\ &\lesssim h^{d-2} \sum_{k\in K} q(\mathrm{b}_k)^2 + \|\nabla p_h^\Gamma\|_{0,\Omega_1\cup\Omega_2}^2 + \sum_{i=1}^2 \sum_{F\in\mathcal{F}_i} h \|[\nabla p_{i,h}]\|_{0,F}^2 \\ &\lesssim h^{d-2} \sum_{k\in K} q(\mathrm{b}_k)^2 + \left[\sup_{v_h\in V_h} \frac{(\mathrm{div}\, v_h, p_h^\Gamma)_0}{\|v_h\|_0} \right]^2 + \sum_{i=1}^2 \sum_{F\in\mathcal{F}_i} h \|[\nabla p_{i,h}]\|_{0,F}^2, \end{aligned} \tag{3.9}$$

where in the last inequality we used Lemma 3.1. It remains to derive a bound for the first term on the right-hand side of (3.9), which is denoted by

$$Q := h^{d-2} \sum_{k \in K} q(\mathrm{b}_k)^2.$$

Recalling that n_h denotes the unit normal vector on Γ_h and $\mathrm{v}_k = \mathrm{v}(F_k)$ for $F_k \in \mathcal{F}_\Gamma^0$, $F_k \subset \widetilde{F}_k$, we define the velocity piecewise *linear* finite element function $u_h \in V_h$:

$$u_h(x) = \begin{cases} q(\mathrm{b}_k) n_h(\mathrm{b}_k) & \text{if } \ x = \mathrm{v}_k, \ k \in K, \\ 0 & \text{at all other vertices in } \mathcal{T}_h^\Gamma. \end{cases}$$

Due to the construction of the set of surface segments $\widetilde{\mathcal{F}}_\Gamma^0$ it follows that u_h is a sum of nodal (vector) basis functions with nonoverlapping supports. From the definition of u_h it follows that

$$Q = h^{d-2} \sum_{k \in K} |u_h(\mathrm{v}_k)|^2 \gtrsim h^{-2} \|u_h\|_0^2. \tag{3.10}$$

Furthermore, on $\tilde{F}_k$ we have that $x \mapsto q(\mathrm{b}_k) u_h(x) \cdot n_h(\mathrm{b}_k)$ is a scalar piecewise linear nonnegative function and on $F_k \subset \tilde{F}_k$,

$$\begin{aligned} \int_{F_k} q(\mathrm{b}_k) u_h(x) \cdot n_h(\mathrm{b}_k) \, dx &\simeq |F_k| q(\mathrm{b}_k) u_h(\mathrm{b}_k) \cdot n_h(\mathrm{b}_k) \\ &\simeq h^{d-1} q(\mathrm{b}_k) u_h(\mathrm{v}_k) \cdot n_h(\mathrm{b}_k), \end{aligned} \tag{3.11}$$

where in the second equivalence we used that v_k is the closest vertex to b_k. Using (3.11) we get

$$\begin{aligned} Q &= h^{d-2} \sum_{k \in K} q(\mathrm{b}_k) u_h(\mathrm{v}_k) \cdot n_h(\mathrm{b}_k) \\ &\simeq h^{-1} \sum_{k \in K} \int_{F_k} q(\mathrm{b}_k) u_h(x) \cdot n_h(\mathrm{b}_k) \, dx \\ &\le h^{-1} \sum_{k \in K} \int_{\tilde{F}_k} q(\mathrm{b}_k) u_h(x) \cdot n_h(\mathrm{b}_k) \, dx \\ &= h^{-1} \sum_{k \in K} \int_{\tilde{F}_k} q(x) u_h(x) \cdot n_h(x) \, dx \\ &\quad + h^{-1} \sum_{k \in K} \int_{\tilde{F}_k} q(\mathrm{b}_k) u_h(x) \cdot \big(n_h(\mathrm{b}_k) - n_h(x)\big) \, dx \\ &\quad + h^{-1} \sum_{k \in K} \int_{\tilde{F}_k} \big(q(\mathrm{b}_k) - q(x)\big) u_h(x) \cdot n_h(x) \, dx \\ &=: h^{-1} \int_{\Gamma_h} q(x) u_h(x) \cdot n_h(x) \, dx + R_1 + R_2. \end{aligned} \tag{3.12}$$

We derive a bound for the term R_1. Let d be the signed distance function to the C^2-smooth surface Γ, hence $\nabla d(x) = n(x)$ for x in a neighborhood of Γ. For $x \in \tilde{F}_k$ we get, using (2.2),

$$\begin{aligned} \|n_h(\mathrm{b}_k) - n_h(x)\| &\le \|n_h(\mathrm{b}_k) - \nabla d(\mathrm{b}_k)\| + \|\nabla d(x) - n_h(x)\| + \|\nabla d(\mathrm{b}_k) - \nabla d(x)\| \\ &\le ch + \|D^2 d\|_\infty \|\mathrm{b}_k - x\| \lesssim h. \end{aligned}$$

Hence, noting $\|u_h\|_{L^\infty(\tilde{F}_k)} \leq |q(\mathrm{b}_k)|$, we obtain

$$|R_1| \lesssim h^{-1} \sum_{k\in K} |\tilde{F}_k||q(\mathrm{b}_k)|\|u_h\|_{L^\infty(\tilde{F}_k)} h \lesssim h^{d-1} \sum_{k\in K} q(\mathrm{b}_k)^2 \simeq h\, Q. \tag{3.13}$$

For deriving a bound for R_2 we use $q(x)-q(\mathrm{b}_k) = \int_{\mathrm{b}_k}^x \nabla q \cdot t\, ds$ and the results in (3.8) and in Lemma 3.1:

$$\begin{aligned} |R_2| &\lesssim \left(h^{-1} \sum_{k\in K} \int_{\tilde{F}_k} \Big| \int_{\mathrm{b}_k}^x \nabla q \cdot t\, ds\Big|^2 dx \right)^{\frac12} \left(h^{-1} \sum_{k\in K} |\tilde{F}_k| \|u_h\|^2_{L^\infty(\tilde{F}_k)} \right)^{\frac12} \\ &\lesssim \left(\|\nabla p_h^\Gamma\|^2_{0,\Omega_1\cup\Omega_2} + \sum_{i=1}^2 \sum_{F\in\mathcal{F}_i} h\|[\nabla p_{i,h}]\|^2_{0,F} \right)^{\frac12} \left(h^{d-2} \sum_{k\in K} q(\mathrm{b}_k)^2 \right)^{\frac12} \\ &\lesssim \left(\sup_{v_h\in V_h} \frac{(\operatorname{div} v_h, p_h^\Gamma)_0}{\|v_h\|_0} + \left(\sum_{i=1}^2 \sum_{F\in\mathcal{F}_i} h\|[\nabla p_{i,h}]\|^2_{0,F} \right)^{\frac12} \right) \sqrt{Q}. \end{aligned} \tag{3.14}$$

To handle the first term on the right-hand side of (3.12) we use integration by parts, Lemma 3.1, and (3.10):

$$\begin{aligned} h^{-1} \int_{\Gamma_h} q(x) u_h(x)\cdot n_h(x)\, dx &= \frac{(-\operatorname{div} u_h, p_h)_0}{\|u_h\|_0} \big(h^{-1}\|u_h\|_0\big) \\ + h^{-1} \sum_{i=1}^2 \int_{\Omega_i} \nabla p_{i,h}\cdot u_h\, dx &\lesssim \left(\sup_{v_h\in V_h} \frac{(\operatorname{div} v_h, p_h)_0}{\|v_h\|_0} + \|\nabla p_h^\Gamma\|_{0,\Omega_1\cup\Omega_2} \right) \\ \big(h^{-1}\|u_h\|_0\big) &\lesssim \left(\sup_{v_h\in V_h} \frac{(\operatorname{div} v_h, p_h)_0}{\|v_h\|_0} + \left(\sum_{i=1}^2 \sum_{F\in\mathcal{F}_i} h\|[\nabla p_{i,h}]\|^2_{0,F} \right)^{\frac12} \right) \sqrt{Q}. \end{aligned} \tag{3.15}$$

Combination of (3.12)–(3.15) yields, for $h \leq h_0$ and $h_0 > 0$ sufficiently small,

$$Q \lesssim \left[\sup_{v_h\in V_h} \frac{(\operatorname{div} v_h, p_h)_0}{\|v_h\|_0} \right]^2 + \sum_{i=1}^2 \sum_{F\in\mathcal{F}_i} h\|[\nabla p_{i,h}]\|^2_{0,F},$$

and using this in (3.9) completes the proof. ∎

The analysis above leads to the main result of this section.

THEOREM 3.3. *There exists $h_0 > 0$ such that for all $h \leq h_0$ the following uniform estimate holds:*

$$\begin{aligned} &\sup_{v_h\in V_h} \frac{(\operatorname{div} v_h, p_h^\Gamma)_0}{\|\rho^{\frac12} v_h\|_0} + \left(\sum_{i=1}^2 \sum_{F\in\mathcal{F}_i} h\|\rho_i^{-\frac12}[\nabla p_{i,h}]\|^2_{0,F} \right)^{\frac12} \\ &\qquad \gtrsim \|\rho^{-\frac12}\nabla p_h^\Gamma\|_{0,\Omega_1\cup\Omega_2} + \rho_{\max}^{-\frac12} h^{-\frac12}\|[p_h^\Gamma]\|_{0,\Gamma_h} \quad \forall\, p_h \in Q_{1,h}\times Q_{2,h}. \end{aligned} \tag{3.16}$$

Proof. Since the sup in the left part of (3.3) is over finite element velocity functions with support in Ω_i, one can scale (3.3) with $\rho_i^{-\frac{1}{2}}$ and add the results for $i = 1, 2$, which yields

$$\sup_{v_h \in V_h} \frac{(\operatorname{div} v_h, p_h^\Gamma)}{\|\rho^{\frac{1}{2}} v_h\|_0} + \left(\sum_{i=1}^{2} \sum_{F \in \mathcal{F}_i} h \|\rho_i^{-\frac{1}{2}} [\nabla p_{i,h}]\|_{0,F}^2 \right)^{\frac{1}{2}} \gtrsim \sum_{i=1}^{2} \|\rho_i^{-\frac{1}{2}} \nabla p_h^\Gamma\|_{0,\Omega_i} = \|\rho^{-\frac{1}{2}} \nabla p_h^\Gamma\|_{0,\Omega_1 \cup \Omega_2} \quad \forall\ p_h \in Q_{1,h} \times Q_{2,h}.$$

Adding this estimate and the one in (3.7) scaled with $\rho_{\max}^{-\frac{1}{2}}$ proves the theorem. ∎

4. Algebraic problem. In this section, we introduce the matrix-vector representation of the finite element problem (2.5). For V_h we use the standard nodal basis denoted by $(\psi_j)_{1 \le j \le m}$, i.e.,

$$V_h \ni u_h = \sum_{j=1}^{m} x_j \psi_j. \tag{4.1}$$

The vector representation of u_h is denoted by $\mathbf{x} = (x_1, \dots, x_m)^T \in \mathbb{R}^m$. In $Q_{i,h}$ we have a standard nodal basis denoted by $(\phi_{i,j})_{1 \le j \le n_i}$, $i = 1, 2$, i.e.,

$$Q_{1,h} \times Q_{2,h} \ni p_h = (p_{1,h}, p_{2,h}) = \left(\sum_{j=1}^{n_1} y_{1,j} \phi_{1,j}, \sum_{j=1}^{n_2} y_{2,j} \phi_{2,j} \right). \tag{4.2}$$

The vector representation of p_h is denoted by $\mathbf{y} = (y_{1,1}, \dots, y_{1,n_1}, y_{2,1}, \dots, y_{2,n_2})^T \in \mathbb{R}^{n_1+n_2}$. We use $\langle \cdot, \cdot \rangle$ and $\|\cdot\|$ for the Euclidean scalar product and norm. The bilinear forms $a(\cdot,\cdot)$, $(\rho\cdot,\cdot)_0$, $b(\cdot,\cdot)$, $j(\cdot,\cdot)$ have corresponding matrix representations, denoted by $A \in \mathbb{R}^{m \times m}, C \in \mathbb{R}^{m \times m}, B \in \mathbb{R}^{(n_1+n_2) \times m}, J \in \mathbb{R}^{(n_1+n_2) \times (n_1+n_2)}$, respectively. The following holds:

$$\begin{aligned} a(u_h, u_h) &= \langle A\mathbf{x}, \mathbf{x} \rangle \quad \forall\ u_h \in V_h, \\ (\rho u_h, u_h)_0 &= \langle C\mathbf{x}, \mathbf{x} \rangle \quad \forall\ u_h \in V_h, \\ b(u_h, p_h^\Gamma) &= \langle B\mathbf{x}, \mathbf{y} \rangle \quad \forall\ u_h \in V_h,\ p_h \in Q_{1,h} \times Q_{2,h}, \\ j(p_h, p_h) &= \langle J\mathbf{y}, \mathbf{y} \rangle \quad \forall\ p_h \in Q_{1,h} \times Q_{2,h}. \end{aligned}$$

The matrices A, C are symmetric positive definite. The matrix J is symmetric positive semidefinite. Let $\mathbf{1} := (1, \dots, 1)^T \in \mathbb{R}^{n_1+n_2}$. From $b(u_h, 1) = 0$ for all $u_h \in V_h$ and $j(1, q_h) = 0$ for all $q_h \in Q_{1,h} \times Q_{2,h}$ it follows that $B^T\mathbf{1} = J\mathbf{1} = 0$ holds. We introduce two mass matrices in the pressure space:

$$\begin{aligned} M &= \operatorname{blockdiag}(M_1, M_2), \quad (M_i)_{k,l} := (\mu_i^{-1} \phi_{i,k}, \phi_{i,l})_{0,\Omega_{i,h}}, \ \ 1 \le k, l \le n_i, \ \ i = 1, 2, \\ \widehat{M} &= \operatorname{blockdiag}(\widehat{M}_1, \widehat{M}_2), \quad (\widehat{M}_i)_{k,l} := (\mu_i^{-1} \phi_{i,k}, \phi_{i,l})_{0,\Omega_i}, \quad 1 \le k, l \le n_i, \ \ i = 1, 2. \end{aligned}$$

For these mass matrices we have the relations

$$\begin{aligned} \langle M\mathbf{y}, \mathbf{y} \rangle &= \|\mu_1^{-\frac{1}{2}} p_{1,h}\|_{0,\Omega_{1,h}}^2 + \|\mu_2^{-\frac{1}{2}} p_{2,h}\|_{0,\Omega_{2,h}}^2 = \|\mu^{-\frac{1}{2}} p_h\|_{0,\Omega_{1,h} \cup \Omega_{2,h}}^2, \\ \langle \widehat{M}\mathbf{y}, \mathbf{y} \rangle &= \|\mu_1^{-\frac{1}{2}} p_{1,h}\|_{0,\Omega_1}^2 + \|\mu_2^{-\frac{1}{2}} p_{2,h}\|_{0,\Omega_2}^2 = \sum_{i=1}^{2} \|\mu_i^{-\frac{1}{2}} p_h^\Gamma\|_{0,\Omega_i}^2 = \|\mu^{-\frac{1}{2}} p_h^\Gamma\|_0^2. \end{aligned}$$

The matrix-vector representation of the discrete problem (2.5) is as follows. First note that $(\mu^{-1}p_h^\Gamma, 1)_0 = 0$ iff $\langle \widehat{M}\mathbf{y}, \mathbf{1}\rangle = 0$. The discrete problem is given as follows: Find $\mathbf{x} \in \mathbb{R}^m$, $\mathbf{y} \in \mathbb{R}^{n_1+n_2}$ with $\langle \widehat{M}\mathbf{y}, \mathbf{1}\rangle = 0$ such that

$$K\begin{pmatrix}\mathbf{x}\\ \mathbf{y}\end{pmatrix} := \begin{pmatrix}A+\tau C & B^T\\ B & -\varepsilon_p J\end{pmatrix}\begin{pmatrix}\mathbf{x}\\ \mathbf{y}\end{pmatrix} = \begin{pmatrix}\mathbf{b}\\ 0\end{pmatrix}, \quad b_j = (f,\psi_j)_0,\ 1 \le j \le m. \tag{4.3}$$

The matrix K of the algebraic system (4.3) is symmetric indefinite. One common approach to solving the system numerically is to exploit the structure of the matrix and to apply a Krylov subspace method with block diagonal preconditioner:

$$\widehat{K} := \begin{pmatrix}A_\tau & 0\\ 0 & Q_\tau\end{pmatrix},$$

where A_τ, Q_τ are both symmetric positive definite matrices and should be chosen as preconditioners of the (1,1)-block $A+\tau C$ and the Schur complement of K, which is given by

$$S_\tau := B(A+\tau C)^{-1}B^T + \varepsilon_p J. \tag{4.4}$$

We refer to [2] for a review of this and other approaches to the numerical solution of saddle point algebraic systems. It is well-known that if A_τ is uniformly (with respect to the relevant parameters) spectrally equivalent to $A+\tau C$ and Q_τ is uniformly spectrally equivalent to S_τ, a preconditioned MINRES method, with preconditioner $\widehat{K}$, applied to the system (4.3) has a high rate of convergence for the whole parameter range. Good preconditioners A_τ for $A+\tau C$ are known, e.g., a multigrid method. In the next section we introduce a Schur complement preconditioner Q_τ.

5. Schur complement preconditioner. In this section we introduce a preconditioner for the Schur complement S_τ.

An ansatz for the Schur complement preconditioner is obtained by looking at the continuous level. It is known that for the Schur complement corresponding to the weak formulation (2.1), with $\mu_1 = \mu_2 = \rho_1 = \rho_2 = 1$, a uniform preconditioner (with respect to τ) is given by

$$\mathcal{Q}_\tau^{-1} := I - \tau\Delta_N^{-1}; \tag{5.1}$$

cf. [23, 19, 21]. Here Δ_N^{-1} is the solution operator of the following Neumann problem: given $f \in L_0^2(\Omega)$, determine $p \in H^1(\Omega) \cap L_0^2(\Omega)$ such that

$$(\nabla p, \nabla q)_0 = (f,q)_0 \quad \forall\ q \in H^1(\Omega). \tag{5.2}$$

The preconditioner (5.1) interpolates between two extreme cases $\tau = 0$ (the Schur complement preconditioner for the *stationary* Stokes problem) and $\tau \to \infty$ (the pressure Poisson problem). We shall use the same interpolation idea on the discrete level and for variable coefficients.

For $\tau = 0$, it is shown in [18] that the preconditioner $Q_0 := \widehat{M} + \varepsilon_p J$ is spectrally equivalent to S_0, i.e., $Q_0 \simeq S_0$, with spectral constants *independent of h, μ and how Γ intersects the triangulation* (note that ρ occurs in neither Q_0 nor S_0).

For the other extreme case, $\tau \to \infty$, a preconditioner for S_τ is constructed by using a suitable discrete version of the Neumann problem (5.2) with variable diffusion coefficient: Determine $p \in H^2(\Omega_1 \cup \Omega_2) \cap L^2_0(\Omega)$ such that

$$\begin{aligned} -\operatorname{div} \rho^{-1} \nabla p &= f \quad \text{in } \Omega_i,\ i = 1, 2, \\ [\rho^{-1} \nabla p \cdot n] &= 0 \quad \text{on } \Gamma, \\ [p] &= 0 \quad \text{on } \Gamma, \\ \nabla p \cdot n_{\partial\Omega} &= 0 \quad \text{on } \partial\Omega. \end{aligned} \tag{5.3}$$

A convergent second order accurate discretization in the XFEM space is obtained by enforcing weak continuity at the interface using the Nitsche method. This discretization was introduced and analyzed in [16]. We recall some results from that paper. One defines the Nitsche-XFEM discretization of the Neumann problem (5.3) as follows: Find $p_h \in Q_h$ such that

$$\begin{aligned} &(\rho^{-1} \nabla p_h, \nabla q_h)_{0,\Omega_1 \cup \Omega_2} - (\{\!\{\rho^{-1} \nabla p_h \cdot n\}\!\}, [q_h])_{0,\Gamma_h} - (\{\!\{\rho^{-1} \nabla q_h \cdot n\}\!\}, [p_h])_{0,\Gamma_h} \\ &\quad + \lambda h^{-1} \rho^{-1}_{\min} [p_h], [q_h])_{0,\Gamma_h} = (f, q_h)_0 \quad \forall\ q_h \in Q_h. \end{aligned} \tag{5.4}$$

Here we used the average $\{\!\{w\}\!\} := \kappa_1 w_1 + \kappa_2 w_2$ with elementwise constants $\kappa_i = \kappa_i(T) = \frac{|\Omega_i \cap T|}{|T|}$ for $T \in \mathcal{T}_h^\Gamma$, $\rho_{\min} = \min\{\rho_1, \rho_2\}$. The parameter $\lambda > 0$ is needed for stabilization. The bilinear form for this discrete problem is given by

$$\begin{aligned} s_h(p_h, q_h) := &(\rho^{-1} \nabla p_h, \nabla q_h)_{0,\Omega_1 \cup \Omega_2} - (\{\!\{\rho^{-1} \nabla p_h \cdot n\}\!\}, [q_h])_{0,\Gamma_h} \\ &- (\{\!\{\rho^{-1} \nabla q_h \cdot n\}\!\}, [p_h])_{0,\Gamma_h} + \lambda h^{-1} \rho^{-1}_{\min} ([p_h], [q_h])_{0,\Gamma_h}. \end{aligned} \tag{5.5}$$

It is known that this bilinear form is uniformly, with respect to h, ρ_i, and the location of Γ_h in the triangulation, equivalent to a simplified one, where the averaging terms are deleted (cf. Lemmata 4 and 5 in [16]):

$$s_h(p_h, p_h) \simeq |\!|\!| p_h |\!|\!|_h^2 := \|\rho^{-\frac{1}{2}} \nabla p_h\|^2_{0,\Omega_1 \cup \Omega_2} + \lambda h^{-1} \rho^{-1}_{\min} \|[p_h]\|^2_{0,\Gamma_h} \tag{5.6}$$

for λ sufficiently large and for all $p_h \in Q_h$. For the corresponding matrix representation we introduce matrices $P, N \in \mathbb{R}^{(n_1+n_2)\times(n_1+n_2)}$ (where P is used to denote Poisson and N denotes Nitsche):

$$\sum_{i=1}^{2} \int_{\Omega_i} \rho_i^{-1} \nabla p_h^\Gamma \cdot \nabla \tilde{p}_h^\Gamma \, dx = \langle P\mathbf{y}, \tilde{\mathbf{y}} \rangle \quad \forall\ p_h, \tilde{p}_h \in Q_{1,h} \times Q_{2,h}, \tag{5.7}$$

$$h^{-1} \rho^{-1}_{\min} ([p_h^\Gamma], [\tilde{p}_h^\Gamma])_{0,\Gamma_h} = \langle N\mathbf{y}, \tilde{\mathbf{y}} \rangle \quad \forall\ p_h, \tilde{p}_h \in Q_{1,h} \times Q_{2,h}. \tag{5.8}$$

Hence, $\langle P\mathbf{y}, \mathbf{y} \rangle + \lambda \langle N\mathbf{y}, \mathbf{y} \rangle = |\!|\!| p_h |\!|\!|_h^2$ holds. For this XFEM discrete Laplacian we use the notation

$$L := P + \lambda N. \tag{5.9}$$

This matrix L is a stable approximation of the part $BC^{-1}B^T$ in the Schur complement S_τ; cf. (4.4). Efficient preconditioners for L are studied in [20] and used in section 7. In section 6 we show that for sufficiently large τ, the Schur complement matrix S_τ is spectrally equivalent to $\frac{1}{\tau} L + \varepsilon_p J$, uniformly in h and the location of Γ_h in the triangulation. Motivated by the structure of the preconditioner on the continuous level,

we use a linear interpolation between the preconditioners for the two extreme cases, $\tau = 0$ and $\tau \to \infty$, similar to (5.1). This leads to the following Schur complement preconditioner:

$$Q_\tau^{-1} := (\widehat{M} + \varepsilon_p J)^{-1} + \tau (L + \tau \varepsilon_p J)^{-1}, \quad \tau \in [0, \infty). \tag{5.10}$$

Experiments in section 7 illustrate the robustness of this preconditioner.

Remark 1. The XFEM discrete Laplacian L in the preconditioner Q_τ^{-1} can be replaced by the matrix corresponding to the bilinear form $s_h(\cdot,\cdot)$ in (5.5). We use the matrix L corresponding to $\|\cdot\|_h^2$ since it is easier to implement and the results are very satisfactory; cf. section 7. Furthermore, the matrix L is always symmetric positive definite, whereas the matrix corresponding to $s_h(\cdot,\cdot)$ is positive definite only for λ sufficiently large.

6. Analysis of the Schur complement preconditioner. We are not able to prove robustness of the preconditioner Q_τ for the whole range $\tau \in [0, \infty)$; cf. Remark 2 below. Although such robustness is observed in numerical experiments, we can only handle the two extreme cases, $\tau \in [0, \kappa_0 c_0] \cup [c_1 \kappa_1 h^{-2}, \infty)$, with $c_i > 0$ given constants and

$$\kappa_0 = \frac{\mu_{\min}}{\rho_{\max}}, \quad \kappa_1 = \frac{\mu_{\max}}{\rho_{\min}},$$

with $\mu_{\max} := \max\{\mu_1, \mu_2\}$, $\mu_{\min} := \min\{\mu_1, \mu_2\}$, $\rho_{\max} := \max\{\rho_1, \rho_2\}$, $\rho_{\min} := \min\{\rho_1, \rho_2\}$. The two parameter ranges $\tau \in [0, \kappa_0 c_0]$ and $\tau \in [c_1 \kappa h^{-2}, \infty)$ are treated in the two subsections below.

In the remainder we assume that the stabilization parameters $\lambda > 0$ and $\varepsilon_p > 0$ are fixed, independent of h, τ, ρ, μ. For two symmetric positive definite matrices A_1, A_2, we use the notation $A_1 \lesssim A_2$, $A_1 \simeq A_2$ to indicate that spectral inequalities are uniform in h, τ, ρ, μ, and the location of the interface in the triangulation. In this section, the constants in the inequalities may depend on c_0, c_1.

6.1. Uniform spectral equivalence for $\tau \in [0, c_0 \kappa_0]$. The results for this case easily follow from the analysis in [18].

LEMMA 6.1. *For $\tau \in [0, c_0 \kappa_0]$ the uniform spectral equivalence*

$$S_\tau \simeq \widehat{M} + \varepsilon_p J$$

holds.

Proof. Note that

$$A \le A + \tau C \lesssim \left(1 + \tau \frac{\rho_{\max}}{\mu_{\min}}\right) A$$

holds. Hence, for $\tau \in [0, c_0 \kappa_0]$ we have $S_\tau \simeq B A^{-1} B^T + \varepsilon_p J = S_0$. The uniform equivalence $S_0 \simeq \widehat{M} + \varepsilon_p J$ is derived in Theorem 6.2 and Lemma 6.3 in [18]. The analysis is based on the LBB stability estimate (3.1). ∎

LEMMA 6.2. *For $\tau \in [0, c_0 \kappa_0]$ the uniform spectral equivalence*

$$Q_\tau \simeq \widehat{M} + \varepsilon_p J$$

holds on the pressure subspace of all $p_h \in Q_{1,h} \times Q_{2,h}$ with $(\mu^{-1} p_h^\Gamma, 1)_0 = 0$.

Proof. The spectral inequality $Q_\tau^{-1} \geq (\widehat{M}+\varepsilon_p J)^{-1}$ follows from the definition of Q_τ. For $\tau > 0$, we also have the chain of inequalities

$$\begin{aligned} Q_\tau^{-1} \lesssim (\widehat{M}+\varepsilon_p J)^{-1} &\Leftrightarrow \ (\tau^{-1}L+\varepsilon_p J)^{-1} \lesssim (\widehat{M}+\varepsilon_p J)^{-1} \\ &\Leftrightarrow \ \widehat{M}+\varepsilon_p J \lesssim \tau^{-1}L+\varepsilon_p J \ \Leftrightarrow \ \widehat{M} \lesssim \tau^{-1}L+\varepsilon_p J. \end{aligned} \tag{6.1}$$

Take $p \in H^1(\Omega_1 \cup \Omega_2)$ with $(\mu^{-1}p, 1)_0 = 0$. We use the orthogonal decomposition $p = p_0 + p_0^\perp$ (orthogonal with respect to $(\mu^{-1}\cdot,\cdot)_0$) with

$$p_0 = \alpha \begin{cases} \mu_1 |\Omega_1|^{-1} & \text{in } \Omega_1, \\ -\mu_2 |\Omega_2|^{-1} & \text{in } \Omega_2, \end{cases}$$

$\alpha \in \mathbb{R}$. We then have $(p_0^\perp, 1)_{0,\Omega_i} = 0$, $i = 1, 2$. Using a trace inequality for $(p_0^\perp)_{|\Omega_i}$ we get

$$\begin{aligned} \|\mu^{-\frac{1}{2}} p_0\|_0^2 &\lesssim \mu_{\min}^{-1} \|[p_0]\|_{0,\Gamma_h}^2 \lesssim \mu_{\min}^{-1} \|[p]\|_{0,\Gamma_h}^2 + \mu_{\min}^{-1} \|[p_0^\perp]\|_{0,\Gamma_h}^2 \\ &\lesssim \mu_{\min}^{-1} \|[p]\|_{0,\Gamma_h}^2 + \mu_{\min}^{-1} \|\nabla p_0^\perp\|_{0,\Omega_1\cup\Omega_2}^2. \end{aligned}$$

Using this and a Poincaré inequality on Ω_i, we get

$$\begin{aligned} \|\mu^{-\frac{1}{2}} p\|_0^2 &= \|\mu^{-\frac{1}{2}} p_0^\perp\|_0^2 + \|\mu^{-\frac{1}{2}} p_0\|_0^2 \lesssim \|\mu^{-\frac{1}{2}} \nabla p_0^\perp\|_{0,\Omega_1\cup\Omega_2}^2 + \|\mu^{-\frac{1}{2}} p_0\|_0^2 \\ &\lesssim \|\mu^{-\frac{1}{2}} \nabla p_0^\perp\|_{0,\Omega_1\cup\Omega_2}^2 + \mu_{\min}^{-1} \|[p]\|_{0,\Gamma_h}^2 = \|\mu^{-\frac{1}{2}} \nabla p\|_{0,\Omega_1\cup\Omega_2}^2 + \mu_{\min}^{-1} \|[p]\|_{0,\Gamma_h}^2. \end{aligned}$$

Hence, for $p_h \in Q_{1,h} \times Q_{2,h}$ with $(\mu^{-1} p_h^\Gamma, 1)_0 = 0$ we obtain

$$\begin{aligned} \langle \widehat{M}\mathbf{y}, \mathbf{y} \rangle = \|\mu^{-\frac{1}{2}} p_h^\Gamma\|_0^2 &\lesssim \|\mu^{-\frac{1}{2}} \nabla p_h^\Gamma\|_{0,\Omega_1\cup\Omega_1}^2 + \mu_{\min}^{-1} \|[p_h^\Gamma]\|_{0,\Gamma_h}^2 \\ &\lesssim \frac{\rho_{\max}}{\mu_{\min}} \|\rho^{-\frac{1}{2}} \nabla p_h^\Gamma\|_{0,\Omega_1\cup\Omega_1}^2 + h \frac{\rho_{\min}}{\mu_{\min}} h^{-1} \rho_{\min}^{-1} \|[p_h^\Gamma]\|_{0,\Gamma_h}^2 \\ &\lesssim \frac{\rho_{\max}}{\mu_{\min}} \Big(\langle (P+N)\mathbf{y}, \mathbf{y} \rangle \Big). \end{aligned}$$

This yields that for $\tau \leq c_0\kappa_0$ the uniform spectral inequality $\widehat{M} \lesssim \frac{1}{\tau} L$ and thus (6.1) holds. ∎

As a direct consequence of the two lemmata above we obtain the following.

COROLLARY 6.3. *Take $\tau \in [0, \kappa_0 c_0]$. The uniform spectral equivalence*

$$Q_\tau^{-\frac{1}{2}} S_\tau Q_\tau^{-\frac{1}{2}} \simeq I$$

holds.

6.2. Uniform spectral equivalence for $\tau \in [c_1\kappa_1 h^{-2}, \infty)$. We introduce

$$\widehat{S}_\tau := \frac{1}{\tau} B C^{-1} B^T + \varepsilon_p J.$$

Note that for $\tau \geq c_1\kappa_1 h^{-2}$ we have

$$\tau C \leq A + \tau C \lesssim \left(h^{-2} \frac{\mu_{\max}}{\rho_{\min}} + \tau \right) C \lesssim \tau C.$$

Therefore,

$$S_\tau \simeq \widehat{S}_\tau \quad \text{for} \quad \tau \geq c_1\kappa_1 h^{-2}. \tag{6.2}$$

LEMMA 6.4. *For $\tau \in (0,\infty)$ the uniform spectral inequality*

$$\widehat{S}_\tau \lesssim \tau^{-1} L + \varepsilon_p J \tag{6.3}$$

holds.

Proof. Note the identities

$$\langle BC^{-1}B^T\mathbf{y},\mathbf{y}\rangle^{\frac{1}{2}} = \max_{\mathbf{x}\in\mathbb{R}^m} \frac{\langle B\mathbf{x},\mathbf{y}\rangle}{\langle C\mathbf{x},\mathbf{x}\rangle^{\frac{1}{2}}} = \max_{u_h\in V_h} \frac{b(u_h,p_h^\Gamma)}{\|\rho^{\frac{1}{2}}u_h\|_0}. \tag{6.4}$$

The trace inequality from [16]

$$\|w\|^2_{L^2(\Gamma_h\cap T)} \le c\big(h_T^{-1}\|w\|^2_{0,T} + h_T\|w\|^2_{1,T}\big) \quad \forall\ w\in H^1(T), \tag{6.5}$$

holds with a constant c independent on how Γ_h intersects the simplex T. Using (6.5) and the finite element inverse estimate $\|u_h\|_{1,T} \le h_T^{-1}\|u_h\|_0$ we get

$$\begin{aligned}
|b(u_h,p_h^\Gamma)| &= \left| \int_{\Gamma_h} u_h\cdot n[p_h^\Gamma]\,ds - \sum_{i=1}^2 \int_{\Omega_i} u_h\cdot\nabla p_h^\Gamma\,dx \right| \\
&\le \|u_h\|_{0,\Gamma_h}\,\|[p_h^\Gamma]\|_{0,\Gamma_h} + \|\rho^{\frac{1}{2}}u_h\|_0\,\|\rho^{-\frac{1}{2}}\nabla p_h^\Gamma\|_{0,\Omega_1\cup\Omega_2} \\
&\lesssim h^{-\frac{1}{2}}\|\rho^{\frac{1}{2}}u_h\|_0\,\rho_{\min}^{-\frac{1}{2}}\|[p_h^\Gamma]\|_{0,\Gamma_h} + \|\rho^{\frac{1}{2}}u_h\|_0\,\|\rho^{-\frac{1}{2}}\nabla p_h^\Gamma\|_{0,\Omega_1\cup\Omega_2}.
\end{aligned}$$

Employing this in (6.4) yields

$$\begin{aligned}
\langle BC^{-1}B^T\mathbf{y},\mathbf{y}\rangle &\lesssim h^{-1}\rho_{\min}^{-1}\|[p_h^\Gamma]\|^2_{0,\Gamma_h} + \|\rho^{-\frac{1}{2}}\nabla p_h^\Gamma\|^2_{0,\Omega_1\cup\Omega_2} \\
&= \langle N\mathbf{y},\mathbf{y}\rangle + \langle P\mathbf{y},\mathbf{y}\rangle \lesssim \langle L\mathbf{y},\mathbf{y}\rangle,
\end{aligned}$$

from which the result (6.3) easily follows. ∎

The proof of the lower spectral bound for $\widehat{S}_\tau$ relies on the LBB stability result (3.16) for the P_2-P_1XFEM pair with ghost penalty stabilization.

LEMMA 6.5. *Take $\tau \in [c_1\kappa_1 h^{-2},\infty)$. There exists $h_0 > 0$ such that for $h \le h_0$ the uniform spectral inequality*

$$\widehat{S}_\tau \gtrsim \frac{\rho_{\min}}{\rho_{\max}}(\tau^{-1}L + \varepsilon_p J)$$

holds.

Proof. Thanks to the relations (6.4) and the definitions of J, P, and N, we rewrite the LBB stability result (3.16) in matrix notation as

$$BC^{-1}B^T + h^{-2}\kappa_1 J \gtrsim P + \frac{\rho_{\min}}{\rho_{\max}}N \gtrsim \frac{\rho_{\min}}{\rho_{\max}}L.$$

The estimate of the lemma now follows for $\tau \gtrsim h^{-2}\kappa_1$. ∎

It remains to show that the proposed preconditioner Q_τ is spectrally equivalent to $\tau^{-1}L + \varepsilon_p J$. This is the assertion of the next lemma.

LEMMA 6.6. *For $\tau \in [c_1\kappa_1 h^{-2},\infty)$ the uniform spectral equivalence*

$$Q_\tau \simeq \tau^{-1}L + \varepsilon_p J$$

holds.

Proof. The spectral inequality $Q_\tau^{-1} \geq (\tau^{-1}L + \varepsilon_p J)^{-1}$ follows from the definition of Q_τ. Observe the chain of the inequalities:

$$\begin{aligned} Q_\tau^{-1} \lesssim (\tau^{-1}L + \varepsilon_p J)^{-1} &\Leftrightarrow \ (\widehat{M} + \varepsilon_p J)^{-1} \lesssim (\tau^{-1}L + \varepsilon_p J)^{-1} \\ &\Leftrightarrow \ \tau^{-1}L + \varepsilon_p J \lesssim \widehat{M} + \varepsilon_p J \ \Leftrightarrow \tau^{-1}L \lesssim \widehat{M} + \varepsilon_p J. \end{aligned} \tag{6.6}$$

Using (6.5) and a standard finite element inverse inequality we get

$$\begin{aligned} h^2\langle L\mathbf{y},\mathbf{y}\rangle &= h^2 \sum_{i=1}^{2} \|\rho^{-\frac{1}{2}}\nabla p_h^\Gamma\|_{0,\Omega_i}^2 + h\lambda\rho_{\min}^{-1}\|[p_h^\Gamma]\|_{0,\Gamma_h}^2 \\ &\lesssim \frac{\mu_{\max}}{\rho_{\min}} \sum_{i=1}^{2} \left(h^2 \|\mu_i^{-\frac{1}{2}}\nabla p_{i,h}\|_{0,\Omega_{i,h}}^2 + h\|\mu_i^{-\frac{1}{2}} p_{i,h}\|_{0,\Gamma_h}^2 \right) \\ &\lesssim \frac{\mu_{\max}}{\rho_{\min}} \sum_{i=1}^{2} \left(h^2 \|\mu_i^{-\frac{1}{2}}\nabla p_{i,h}\|_{0,\Omega_{i,h}}^2 + \|\mu_i^{-\frac{1}{2}} p_{i,h}\|_{0,\Omega_{i,h}}^2 \right) \\ &\lesssim \frac{\mu_{\max}}{\rho_{\min}} \sum_{i=1}^{2} \|\mu_i^{-\frac{1}{2}} p_{i,h}\|_{0,\Omega_{i,h}}^2 \lesssim \frac{\mu_{\max}}{\rho_{\min}} \langle M\mathbf{y},\mathbf{y}\rangle. \end{aligned}$$

In Lemma 6.3 in [18] the uniform spectral equivalence $M \simeq \widehat{M} + \varepsilon_p J$ is shown. Combining these results we get, for $\tau \geq c_1\kappa_1 h^{-2}$,

$$\tau^{-1}L \lesssim h^2 \frac{\rho_{\min}}{\mu_{\max}} L \lesssim M \simeq \widehat{M} + \varepsilon_p J,$$

which proves the last estimate in (6.6). ∎

As a direct consequence of Lemmata 6.4–6.6 and (6.2) above we obtain the following.

COROLLARY 6.7. *Take $\tau \in [c_1\kappa_1 h^{-2}, \infty)$. Then the uniform spectral equivalence*

$$\frac{\rho_{\min}}{\rho_{\max}} I \lesssim Q_\tau^{-\frac{1}{2}} S_\tau Q_\tau^{-\frac{1}{2}} \lesssim I$$

holds.

Remark 2. The analysis in this section proves the robustness of the Schur complement preconditioner Q_τ only for $\tau \in [0, c_0\kappa_0] \cup [c_1\kappa_1 h^{-2}, \infty)$. Clearly, these results are less satisfactory in two respects. First, we are not able to prove robustness for the whole range $\tau \in [0, \infty)$ (under assumptions on the viscosity and density ratio). Second, the "constants" τ_i used in the intervals $[0, c_0\kappa_0]$, $[c_1\kappa_1 h^{-2}, \infty)$ depend on the problem parameters μ_i, ρ_i.

We comment on the first issue. Even if we restrict to the case $\frac{\rho_1}{\rho_2} \sim 1$, $\frac{\mu_1}{\mu_2} \sim 1$ we are not able to prove robustness for the whole τ range. The difficulty that we encounter is related to the implicit coupling of diffusion A and reaction C terms in the Schur complement matrix, $B(A + \tau C)^{-1}B^T$. While the limiting cases $\tau \downarrow 0$ and $\tau \to \infty$ are amenable to analysis, the intermediate τ range is not easy to analyze. For the simpler case of a smooth unsteady Stokes problem *without* interface, two approaches are known in the literature which help to extend the robustness property of preconditioning to all $\tau \in [0, \infty)$. The first one from [23] uses an interpolation argument based on the H^2 regularity of the differential problem, which the interface

Stokes *interface* problem that we consider does not possess. The second approach from [21] uses a uniform boundedness of the Bogovski operator in the differential setting and requires the construction of a uniformly bounded Fortin projector to the finite element space. This approach requires that the finite pair that is used is LBB stable. However, the pair (V_h, Q_h) that we consider is *not* LBB stable. Moreover, if the latter approach is applied to the Stokes interface problem (1.1) one would need a uniform boundedness of the Bogovski operator in weighted norms, a result that we are not aware of. Therefore, we are not able to extend these known approaches for a smooth Stokes problem to the Stokes interface problem and hence we cannot prove robustness of the preconditioner for all $\tau \in [0, \infty)$.

Related to the second issue we note the following. The ghost penalty terms in the standard inf-sup condition (3.1) for the Stokes problem and the alternative inf-sup condition (3.16) for the Darcy problem have different scaling with respect to problem parameters. Since both of these inequalities are applied to analyze (2.5), this results in the dependence of κ_0 and κ_1 on the ratio between diffusion and density coefficients. One may attempt to remove this dependence by the design of the ghost penalty term in (2.5) which accounts for both μ-s and ρ-s. However, this makes the stabilization dependent on the time step, which is an undesirable property. We did not study this option.

7. Numerical experiments.

7.1. Discretization error. In [17] the P_2-P_1XFEM pair with ghost penalty stabilization is considered only for a *stationary* Stokes interface problem, and it is shown that the method then has optimal discretization error bounds. In this section we consider a *time-dependent* Stokes problem with a pressure solution that is discontinuous across a stationary interface and illustrate that the proposed discretization has (optimal) second order accuracy. We consider the unsteady Stokes equations on the domain $\Omega = [-1, 1]^3$ with constant density and viscosity coefficients $\rho = \mu = 1$. We take the following analytical solutions:

$$u_a(t, x) = e^{-\|x\|^2} \begin{pmatrix} -x_2 \\ x_1 \\ 0 \end{pmatrix} (1 - e^{-t}), \tag{7.1}$$

$$p_a(t, x) = x_1^3(1 - e^{-t}) + \begin{cases} 1, & x \in \Omega_1, \\ 0, & x \in \Omega_2, \end{cases} \tag{7.2}$$

where $\Omega_1 = \{x \in \Omega : \|x\| < r_\Gamma\}$, $\Gamma = \{x \in \Omega : \|x\| = r_\Gamma\}$, $\Omega_2 = \Omega \setminus \overline{\Omega}_1$ with $r_\Gamma = 2/3$. A force $f = f_\Omega + \hat{f}_\Gamma$ with a body force f_Ω and interface force $\hat{f}_\Gamma(v) := \sigma \int_\Gamma v \cdot n_\Gamma \, ds$ with $\sigma = 1$ is imposed on the right-hand side in (2.1) such that the unsteady Stokes equations have as solution $u = u_a$ and $p = p_a$. The choice of the velocity field u_a is consistent with a stationary interface Γ, since $u \cdot n_\Gamma = 0$ holds. Note that instead of a surface tension force, where the interface curvature has to be approximated, the artificial surface force $\hat{f}_\Gamma$ has been chosen for which a second order discretization is available. The discretization of the surface tension force is crucial for the convergence order of two-phase flow simulations (cf. [14, 12]), but these effects are not studied here.

In the initial triangulation $\mathcal{T}_{h_0}$, i.e., refinement level 0, the domain is subdivided into $4 \times 4 \times 4$ cubes each consisting of 6 tetrahedral elements. For the experiments the mesh is successively uniformly refined, halving the mesh size h in each refinement step. Hence, the mesh for refinement level 3 consists of $32 \times 32 \times 32 \times 6$ tetrahedral

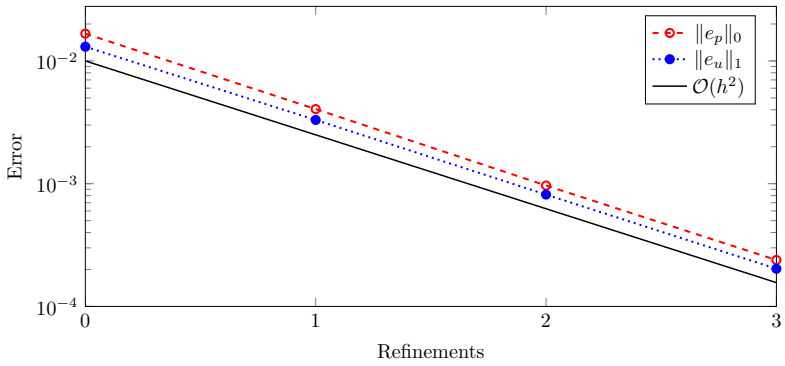

FIG. 2. *Discretization errors for simultaneous temporal and spatial refinement.*

elements. For the piecewise linear approximation Γ_h of the interface Γ we use the zero level of the piecewise linear interpolation $I_{h/2}\, d_\Gamma$ on $\mathcal{T}_{h/2}$ of the signed distance function d_Γ to Γ. For time discretization we apply the implicit Euler method, with a uniform time step denoted by Δt. The simulations are performed until the final time $t = t_f := 0.1$ is reached. The coarsest time step size is $\Delta t = 0.01$. For each spatial refinement step the time step size Δt is divided by four. This results in a time step size $\Delta t = 1.5625 \cdot 10^{-4}$ on refinement level 3 and requires 640 time steps to reach $t = t_f$. In each time step we use the finite element discretization described in section 2, with a constant stabilization parameter value $\varepsilon_p = 0.1$. Figure 2 shows the convergence results for the pressure error $e_p(x) = p(x, t_f) - p_h(x, t_f)$ with respect to the L^2-norm and velocity error $e_u(x) = u(x, t_f) - u_h(x, t_f)$ with respect to the H^1-norm for $t_f = 0.1$. The results show a clear second order convergence behavior. In further experiments (not presented here) one observes that the velocity L^2 error $\|e_u\|_0$ also has a second order convergence behavior. This can be explained by the fact that the time discretization error dominates the total error.

7.2. Schur complement preconditioner. We consider the preconditioner

$$Q_\tau^{-1} := \left(\widehat{M} + \varepsilon_p J\right)^{-1} + \tau \left(L + \tau \varepsilon_p J\right)^{-1} \tag{7.3}$$

with $\tau = 1/\Delta t$. Spectral condition numbers $\kappa(Q_\tau^{-1} S_\tau) := \lambda_{\max}(Q_\tau^{-1} S_\tau)/\lambda_{\min}(Q_\tau^{-1} S_\tau)$ of the preconditioned Schur complement are shown in Table 1 for varying mesh size h and time step size Δt. We use the parameter values $\varepsilon_p = 0.1$ (stabilization parameter in discretization method) and $\lambda = 1$ (parameter in Nitsche-XFEM discretization; cf. (5.9)). To obtain the eigenvalues MATLAB's `eigs` was utilized. Different from the previous experiment, to reduce memory requirements in the MATLAB computation an adaptive refinement around the interface Γ was applied. Refinement level $l = 0$ denotes the unrefined mesh, which is the same as in the previous experiment, whereas $l = 1, 2$ means that the mesh is refined once/twice around the interface. The results reveal very strong robustness for $\Delta t \lesssim 10^{-5}$. For larger Δt there is a dependence of the condition number on the refinement level l. For the condition number computations, more refinement levels could not be used due to memory limitations. For a similar two-dimensional experiment on uniformly refined grids up to level $l = 3$ (not presented here) we observed a robust behavior of the condition numbers for the whole range of Δt and l. In the next experiment iteration numbers for the preconditioned system are investigated, which can also be computed on finer grids.

TABLE 1

Spectral condition numbers of preconditioned Schur complement $Q_\tau^{-1}S_\tau$ for fixed $\varepsilon_p = 0.1$, $\lambda = 1$, and varying time step size Δt and mesh width h.

	$\Delta t = 10^{-1}$	$\Delta t = 10^{-3}$	$\Delta t = 10^{-5}$	$\Delta t = 10^{-7}$	$\Delta t = 10^{-9}$
$l = 0$	49.88	25.45	20.99	20.94	20.94
$l = 1$	49.52	25.63	21.33	21.14	21.13
$l = 2$	91.19	79.90	19.59	16.20	16.15

TABLE 2

Iteration numbers of MINRES with constant $\varepsilon_p = 0.1$, $\lambda = 1$, and varying step size Δt and mesh width h.

	$\Delta t = 10^{-1}$	$\Delta t = 10^{-3}$	$\Delta t = 10^{-5}$	$\Delta t = 10^{-7}$	$\Delta t = 10^{-9}$
$l = 0$	64	46	41	41	42
$l = 1$	64	53	50	53	53
$l = 2$	63	52	47	47	49
$l = 3$	64	49	45	44	45

Table 2 shows the iteration numbers for MINRES, with a relative tolerance of 10^{-6}, using the proposed Schur complement preconditioner applied to the previous defined system. Here, again Δt and the mesh size are varied. The part $(\widehat{M} + \varepsilon_p J)^{-1}$ in the Schur complement preconditioner is approximated by a Jacobi preconditioned CG solver with relative tolerance 10^{-4}. The part $(L + \tau\varepsilon_p J)^{-1}$ is approximated by a symmetric Gauss–Seidel preconditioned CG solver with relative tolerance 10^{-4}. A symmetric Gauss–Seidel preconditioned CG solver with relative tolerance 10^{-2} is used as preconditioner A_τ for the $(1,1)$-block $A + \tau C$. The rather small relative tolerance 10^{-4} in the CG solvers is needed to preserve the symmetry of the Schur complement preconditioner. For values larger than that, MINRES sometimes diverges due to symmetry loss.

The results are in accordance with the observations made in the previous experiment, but we observe a stronger robustness with respect to variations in mesh size.

Remark 3. The Jacobi preconditioned CG method is an efficient solver for the linear system with matrix $\widehat{M}+\varepsilon_p J$, because this matrix is uniformly spectrally equivalent to the well-conditioned mass matrix M. An efficient robust solver for the systems with matrix $L + \tau\varepsilon_p J$ is much more difficult. For very large τ values (i.e., very small Δt) this matrix has an extremely large condition number. Furthermore, the matrix J has a very large kernel. For not too small values of Δt the performance of the symmetric Gauss–Seidel preconditioned CG method is acceptable. As an example, for $\Delta t = 10^{-3}$ the iteration counts for the inner CG solver for $l = 0, 1, 2, 3$ are $42, 26, 22, 24$, respectively. Note that the system with matrix $L+\tau\varepsilon_p J$ has dimension equal to the number of pressure unknowns, which is much smaller than the number of velocity unknowns. Hence, somewhat higher iteration counts for solving the system with matrix $L+\tau\varepsilon_p J$ are still acceptable in view of the total costs of one preconditioned MINRES iteration. For very small Δt the counts are no longer acceptable. For example, for $\Delta t = 10^{-9}$ and $l = 0, 1, 2, 3$ the iteration numbers are $58, 148, 455, 1480$, respectively. We are not aware of a solver for the system with matrix $L + \tau\varepsilon_p J$ that is robust and efficient for the whole h and Δt range. One possible approach, which turned out to be rather promising in our experiments, is to use a special subspace decomposition as in [27], in which information on the kernel of J is used.

TABLE 3

Spectral condition numbers of the preconditioned Schur complement $Q_\tau^{-1}S_\tau$ for fixed $l = 1$, $\Delta t = 10^{-5}$, and varying λ and ε_p.

	$\varepsilon_p = 10^{-4}$	$\varepsilon_p = 10^{-3}$	$\varepsilon_p = 10^{-2}$	$\varepsilon_p = 10^{-1}$	$\varepsilon_p = 1$	$\varepsilon_p = 10$
$\lambda = 0.01$	2143	2132	2112	2104	2103	2103
$\lambda = 0.1$	219	215.5	211.9	210.5	210.3	210.3
$\lambda = 1$	27.24	24.68	22.36	21.33	21.08	21.04
$\lambda = 10$	19.06	20.21	20.18	20.12	20.11	20.11
$\lambda = 100$	143	111.1	105.7	108.5	111.2	112.6

TABLE 4

Iteration numbers of MINRES with $\Delta t = 10^{-3}$, $\mu_2 = \rho_2 = \rho_1 = 1$, $\varepsilon_p = 0.1$, $\lambda = 1$, and varying mesh size h and viscosity μ_1.

	$\mu_2/\mu_1 = 10^{-5}$	10^{-3}	10^{-1}	1	10	10^3	10^5
$l = 0$	44	46	47	46	46	47	47
$l = 1$	55	53	54	53	52	53	52
$l = 2$	51	50	52	52	53	52	52
$l = 3$	54	52	48	49	51	49	49

In the following experiment again the spectral condition numbers are studied, but now for a fixed mesh refinement level $l = 1$ and time step size $\Delta t = 10^{-5}$ and varying stabilization parameter ε_p and Nitsche parameter λ. We recall that ε_p is used in the FE method for the original time-dependent Stokes problem, while λ appears in the definition of the preconditioner and hence can be chosen to optimize the algebraic solver performance. The results are presented in Table 3. Robustness with respect to ε_p can be observed. The results show that in the preconditioner the Nitsche term in (5.9) is essential. One can observe that for $\lambda \to 0$ and thus a vanishing penalization of discontinuities at the interface, the condition number increases very strongly. On the other hand, for $\lambda \gtrsim 10$ one can observe the effect of overpenalization, i.e., a too strong weight is laid on the continuity across the interface.

Overall, the preconditioner shows robustness for the case of constant coefficients $\rho_{1,2} = \mu_{1,2} \simeq 1$. The robustness holds for a certain range of Nitsche parameter values $\lambda \in [1, 10]$.

7.3. Jumping coefficients. In this experiment we study the performance of the preconditioner with respect to variations in the coefficients ρ_i and μ_i. We show results for the iteration numbers of MINRES for the discrete problem on uniform meshes and use the same settings as described in section 7.2. Table 4 shows the iteration numbers of MINRES for varying mesh size h and viscosity ratio μ_2/μ_1. The iteration numbers are almost constant for the different viscosity ratios and hence the preconditioner shows a strong robustness with respect to jumps in the viscosities.

We also consider the robustness with respect to jumps in density for a case with a constant viscosity. Table 5 shows the results for varying mesh size and density ratios. We observe a very mild dependence of the iteration numbers for ratios $\rho_{\max}/\rho_{\min} \in [10^{-5}, 10]$ but a significant increase for $\rho_{\max}/\rho_{\min} \geq 10^3$, especially on the largest refinement level $l = 3$. For the case with extremely large density jumps the behavior

TABLE 5
Iteration numbers of MINRES with $\Delta t = 10^{-3}$, $\rho_1 = \mu_1 = \mu_2 = 1$, $\varepsilon_p = 0.1$, $\lambda = 1$, and varying mesh size h and density ρ_2.

	$\rho_2/\rho_1 = 10^{-5}$	10^{-3}	10^{-1}	1	10	10^3	10^5
$l = 0$	60	73	61	46	45	67	269
$l = 1$	70	79	65	53	53	101	433
$l = 2$	72	83	66	52	54	133	595
$l = 3$	88	87	68	49	53	153	634

TABLE 6
Iteration numbers of MINRES with $\Delta t = 10^{-3}$, $\rho_1 = \mu_1 = \mu_2 = 1$, $\varepsilon_p = 0.1$, and varying mesh size h and density ρ_2 for the element-dependent Nitsche parameter λ_T.

	$\rho_2/\rho_1 = 10^{-5}$	10^{-3}	10^{-1}	1	10	10^3	10^5
$l = 0$	69	71	61	48	46	50	46
$l = 1$	80	80	66	54	52	60	65
$l = 2$	85	85	66	51	53	54	54
$l = 3$	92	89	68	50	50	54	55

can be improved using an idea from [17]. We take an element-dependent Nitsche parameter

$$\lambda_T = \rho_{\min}\{\rho^{-1}\}\left(D + C\frac{\gamma_T}{\alpha_T}\right) \tag{7.4}$$

with constants $D > 0$ and $C > 1$. Here, the averaging operator is defined as $\{a\} := \kappa_1 a_1 + \kappa_2 a_2$ with the element-dependent weights

$$\kappa_1|_T = \frac{\rho_2^{-1}\alpha_{1,T}}{\rho_1^{-1}\alpha_{2,T} + \rho_2^{-1}\alpha_{1,T}}, \qquad \kappa_2|_T = \frac{\rho_1^{-1}\alpha_{2,T}}{\rho_1^{-1}\alpha_{2,T} + \rho_2^{-1}\alpha_{1,T}},$$

and $\alpha_{i,T} := |T \cap \Omega_i|/h_T^3$ with h_T the diameter of element $T \in \mathcal{T}_h$. Such a harmonic weighting is also used in [1] for a Nitsche-type discretization of a Poisson interface problem. The other terms in (7.4) are $\alpha_T := \alpha_{1,T} + \alpha_{2,T}$ and $\gamma_T := |\Gamma \cap T|/h_T^2$. The previous experiment was repeated, but now with an element-dependent Nitsche parameter $\lambda = \lambda_T$. Table 6 shows the corresponding iteration numbers, where the free parameters in λ_T are chosen as $D = 0.5$ and $C = 1.5$. The iteration numbers for the element-dependent Nitsche parameter λ_T are comparable to those obtained for the constant Nitsche parameter λ for the case of a small or moderate density ratio $\rho_{\max}/\rho_{\min} \in [10^{-5}, 10]$ but are also very robust for large density ratios $\rho_{\max}/\rho_{\min} \geq 10^3$. For the extreme case of $\rho_2/\rho_1 = 10^5$ and $l = 3$ the iteration number is reduced by a factor of 11 when taking λ_T instead of λ while the computational effort for the application of the Schur complement preconditioner stays essentially the same.

8. Conclusions. In this paper we studied the efficient preconditioning of linear saddle point systems resulting from the finite element discretization, with the pair P_1-XFE (for pressure) and P_2 (for velocity), of a *quasi-stationary* Stokes *interface* problem. In the discretization a ghost penalty pressure stabilization technique known from the literature was used. The resulting discretization has optimal approximation properties and is robust with respect to nonalignment of the (approximate)

interface in the triangulation. We introduced and analyzed a new Schur complement preconditioner. Numerical experiments illustrate the performance of this preconditioner, in particular its robustness with respect to variation in h, τ, the position of the interface in the triangulation, and the viscosity quotient μ_1/μ_2. Using a suitable element-dependent Nitsche parameter leads to robustness with respect to the density quotient ρ_1/ρ_2, too. We mention two topics that deserve further investigation. First, the theoretical robustness analysis covers only the extreme ranges for the problem parameter τ, namely, τ sufficiently small ($\tau \in [0, c_0\kappa_0]$) or τ sufficiently large ($\tau \in [c_1\kappa_1 h^{-2}, \infty)$). It is not clear how to analyze the intermediate τ range. Second, in the Schur complement preconditioner linear systems with matrix $L + \tau\varepsilon_p J$ have to be solved approximately. For "very large" τ values the efficient solution of these systems turns out to be difficult, and the development of an appropriate preconditioner for this matrix deserves further attention.

REFERENCES

[1] N. Barrau, R. Becker, E. Dubach, and R. Luce, *A robust variant of NXFEM for the interface problem*, C. R. Math., 350 (2012), pp. 789–792.

[2] M. Benzi, G. H. Golub, and J. Liesen, *Numerical solution of saddle point problems*, Acta Numer., 14 (2005), pp. 1–137.

[3] M. Bercovier and O. Pironneau, *Error estimates for finite element method solution of the Stokes problem in the primitive variables*, Numer. Math., 33 (1979), pp. 211–224.

[4] E. Burman, *La pénalisation fantôme*, C. R. Math., 348 (2010), pp. 1217–1220.

[5] E. Burman, S. Claus, P. Hansbo, M. Larson, and A. Massing, *CutFEM: Discretizing geometry and partial differential equations*, Internat. J. Numer. Methods. Engrg., 104 (2015), pp. 472–501.

[6] E. Burman and P. Hansbo, *Fictitious domain finite element methods using cut elements:* II. *A stabilized Nitsche method*, Appl. Numer. Math., 62 (2012), pp. 328–341.

[7] L. Cattanneao, L. Formaggio, G. Iori, A. Scotti, and P. Zunino, *Stabilized extended finite elements for the approximation of saddle point problems with unfitted interfaces*, Calcolo, (2014), http://dx.doi.org/10.1007/s10092–014–0109–9.

[8] Y. C. Chang, T. Y. Hou, B. Merriman, and S. Osher, *A level set formulation of Eulerian interface capturing methods for incompressible fluid flows*, J. Comput. Phys., 124 (1996), pp. 449–464.

[9] A. Demlow and M. A. Olshanskii, *An adaptive surface finite element method based on volume meshes*, SIAM J. Numer. Anal., 50 (2012), pp. 1624–1647.

[10] T. Fries and T. Belytschko, *The generalized/extended finite element method: An overview of the method and its applications*, Internat. J. Numer. Methods Engrg., 84 (2010), pp. 253–304.

[11] V. Girault and P. A. Raviart, *Finite Element Methods for Navier-Stokes Equations*, Springer, Berlin, 1986.

[12] J. Grande, *Finite element discretization error analysis of a general interfacial stress functional*, SIAM J. Numer. Anal., 53 (2015), pp. 1236–1255.

[13] S. Gross and A. Reusken, *An extended pressure finite element space for two-phase incompressible flows with surface tension*, J. Comput. Phys., 224 (2007), pp. 40–58.

[14] S. Gross and A. Reusken, *Finite element discretization error analysis of a surface tension force in two-phase incompressible flows*, SIAM J. Numer. Anal., 45 (2007), pp. 1679–1700.

[15] S. Gross and A. Reusken, *Numerical Methods for Two-Phase Incompressible Flows*, Springer, Berlin, 2011.

[16] A. Hansbo and P. Hansbo, *An unfitted finite element method, based on Nitsche's method, for elliptic interface problems*, Comput. Methods Appl. Mech. Engrg., 191 (2002), pp. 5537–5552.

[17] P. Hansbo, M. Larson, and S. Zahedi, *A cut finite element method for a Stokes interface problem*, Appl. Numer. Math., 85 (2014), pp. 90–114.

[18] M. Kirchhart, S. Gross, and A. Reusken, *Analysis of an XFEM discretization for stokes interface problems*, SIAM J. Sci. Comput., 38 (2016), pp. A1019–A1043.

[19] G. M. Kobelkov and M. A. Olshanskii, *Effective preconditioning of Uzawa type schemes for a generalized Stokes problem*, Numer. Math., 86 (2000), pp. 443–470.

[20] C. Lehrenfeld and A. Reusken, *Optimal preconditioners for Nitsche-XFEM discretizations of interface problems*, Numer. Math. (2016), DOI:10.1007/s00211-016-0801-6.
[21] K.-A. Mardal, J. Schöberl, and R. Winther, *A uniformly stable Fortin operator for the Taylor-Hood element*, Numer. Math., 123 (2013), pp. 537–551.
[22] A. Massing, M. Larson, A. Logg, and M. Rognes, *A stabilized Nitsche fictitious domain method for the Stokes problem*, SIAM J. Sci. Comput., 61 (2014), pp. 604–628.
[23] M. A. Olshanskii, J. Peters, and A. Reusken, *Uniform preconditioners for a parameter dependent saddle point problem with application to generalized Stokes interface equations*, Numer. Math., 105 (2006), pp. 159–191.
[24] S. Osher and R. P. Fedkiw, *Level set methods: An overview and some recent results*, J. Comput. Phys., 169 (2001), pp. 463–502.
[25] H. Sauerland and T. Fries, *The extended finite element method for two-phase and free-surface flows: A systematic study*, J. Comput. Phys., 230 (2011), pp. 3369–3390.
[26] H. Sauerland and T. Fries, *The stable XFEM for two-phase flows*, Comput. & Fluids, 87 (2013), pp. 41–49.
[27] J. Schöberl, *Robust multigrid preconditioning for parameter-dependent problems* I*: The Stokes-type case*, in Multigrid Methods V, Springer, Berlin, 1998, pp. 260–275.
[28] A.-K. Tornberg and B. Engquist, *A finite element based level-set method for multiphase flow applications*, Comput. Visual. Sci., 3 (2000), pp. 93–101.